Combining multi-step imprinting with the in-plane compression method

Miyata, Tsuyoshi
Department of Mechanical and Aerospace Engineering, Kyushu University

Tokumaru, Kazuki
Department of Mechanical Engineering Graduate School of, Kyushu University

Tsumori, Fujio
Department of Mechanical Engineering, Kyushu University

出版情報：Japanese Journal of Applied Physics. 59 (SI), pp.SIIJ07-, 2020-06-01. 応用物理学会
バージョン：
権利関係：

Combining multi-step imprinting with the in-plane compression method

Tsuyoshi Miyata[1], Kazuki Tokumaru[2], and Fujio Tsumori*[3],

[1]Dept. of Mechanical and Aerospace Engineering, Kyushu Univ., Fukuoka, 819-0395, Japan

[2]Dept. of Mechanical Engineering Graduate School of, Kyushu University, Fukuoka, 819-0395, Japan

[3]Dept. of Mechanical Engineering, Kyushu University, Fukuoka, 819-0395, Japan

Phone / Fax: +81-92-802-3208 / 0001, e-mail: tsumori@mech.kyushu-u.ac.jp

Abstract

In this study, a micro patterning process is proposed and developed in order to obtain various functional properties on the surface of an object. Nano imprint lithography (NIL) has recently been the focus of much attention, because of advantages such as high accuracy, low cost, and ease of operation. However, problems can occur during demolding when using this method, such as the destruction of high-aspect patterns during the process. It is also, almost impossible to form an over-hanging pattern. In order to overcome these problems, we propose a multi-step imprinting process with an in-plane compression method. A hierarchical multi-scale pattern can be produced using multi-step imprinting, and the aspect ratio of the imprinted pattern can be increased by using the in-plane compression method. A hierarchical multi-scale pattern with a high aspect ratio was produced by combining the two methods. The effectiveness of the proposed method is demonstrated by the results of the experimentation.

1. Introduction

The production of functional surfaces that mimic those produced by biology has been the focus of considerable amounts of investigation by several research groups in recent years[1-10]. The micro-patterns that are found on functional natural surfaces are the focus of this study. The most well-known example of such micro-patterning is seen on the surface of lotus leaves, where the structure renders the leaves hydrophobic because of the hierarchical multi-scale pattern on the surface. The wing of the *Morpho* butterfly is another famous example, which is a vivid blue structural color. However, it is difficult to produce surface structures that mimic those observed in nature. The aim of this study is therefore to develop a method that can be used to form bio-mimicking hierarchical multi-scale patterns.

Nanoimprint lithography (NIL) was the method chosen for the generation of microstructures on the surface of an object in this study. NIL is a microfabrication technology that was first proposed by S. Chou with the objective of transferring a fine pattern onto a resin using a mold [11–15]. NIL is classified into 2 categories; thermal imprinting and UV imprinting, for which thermo-plastic resin and UV-curable resin are used, respectively. NIL is suitable for mass production because of its low cost and simple manufacturing process. Thermal imprinting was selected to form

various kinds of materials in this study, the schematics of which are shown in Fig. 1. Other imprinting methods were also developed for use in this study; “micro powder imprinting”, “multi-layer imprinting”, and the “in-plane compression method”, were combined to fabricate the complicated bio-mimicking micro-patterns.

Micro powder imprinting (μPI) [16–26] was initially used in this study. Thermo-plastic polymer materials are generally used for thermal imprinting; however, an imprinting process using inorganic materials that can be utilized to fabricate ceramic products with fine patterns was developed for this study. Compound materials, that comprised a mixture of an inorganic nano-powder material and a binder polymer, were used to produce a sheet that could be imprinted using a mold. The sheet was subsequently heated, both to remove the binder polymer and for sintering. This μPI is an extension of NIL technology to include powder metallurgy, and could be used for transferring patterns onto ceramics and glass materials. We have applied the process to improve the solid oxide fuel cell, which is constructed using ceramic materials.

A different imprinting process using multi-layered materials was also investigated in this study, as shown in Fig. 2. In this process, two or more sheets are used as a starting material. A pattern can be transferred onto both the surface layer and the interface between the layers by imprinting both sheets simultaneously. In this method, the mold pattern is transcribed directly onto the surface layer, and the interface between the layers is deformed during the process. Pure polymer is used as the upper layer and ceramic compound as the lower layer. The upper layer can therefore be used as a sacrificial layer; it is removed during heating and before sintering so that the interfacial pattern becomes the surface pattern of the sintered sample.

The final method investigated in this study is the “in-plane compression method.” Various interfacial patterns with a high aspect ratio can be fabricated using this method. Details of this process used for construction will be given in the section concerning fabrication.

Several studies have reported the formation of hierarchical patterns during imprinting [27, 28]. In these cases, finer patterns were transcribed onto the top of rough patterns, as shown in Fig. 3(a). We propose that a fine pattern can be constructed whole on top of a rough pattern. However, it is extremely difficult to imprint a pattern onto the vertical wall of a rough pattern, so a method that could be used to form a fine pattern and subsequently imprint a rougher pattern was required. In order to avoid the occurrence of distortion that can occur in the fine pattern during a second imprinting as seen in Fig. 3(b), an in-plane compression method is proposed. The method proposed is demonstrated in Fig. 3(c), in which the fine pattern is deformed in the manner required using the in-plane compression method.

2. Materials

An alumina composite was prepared as a starting material for this study. The method used

to prepare the sheets is demonstrated in Fig. 4. First, alumina powder, poly-vinyl alcohol (PVA) (with a polymerization degree of 500 and a saponification degree from 86.0 to 90.0 mol %, FUJFILM Wako Pure Chemical Corporation), and glycerin were mixed with pure water. Alumina powder (TM-DAR, TAIMEI CHEMICALS) with an average particle size of 0.1 μm and a purity of 99.99 % was used. PVA was utilized as a binder, and glycerin was added as a plasticizer. The doctor blade method was then used to apply the prepared slurry onto a PET substrate, forming a sheet of uniform thickness [29]. The applied slurry was then placed in an oven and heated at 70 °C for 900 s so that any water in the slurry could evaporate, and a composite sheet with a thickness of between 120 and 130 μm was obtained. The sheet was then divided into 20 mm squares in order to fit into the container used for imprinting.

A sacrificial layer was used during the multi-step imprinting process in this study, as described in the following section [15, 16, 30, 31]. PVA and Polymethyl Methacrylate (PMMA) (with an average molecular weight of 350 k, Sigma-Aldrich) solutions were prepared in order to compare the effects of the material used to construct the protective layer on the pattern produced at the interface during imprinting. The PVA was prepared in a 20 mass% aqueous solution. Food coloring (Kyoritsu-foods) was added for easy observation with an optical microscope. The PMMA was dissolved in acetone at 9 mass%. 1 mass% of Polyethylene Oxide (ALKOX EP-10, Meisei Chemical Works) was also added to increase the viscosity of the solution.

Dynamic mechanical analysis (DMA) was then performed in order to obtain the viscoelastic properties of these materials. The obtained data is shown in Fig. 5. The storage modulus of the alumina compound was found to be 122.0 MPa with a loss modulus of 50.9 MPa, the storage modulus of the PVA was 29.6 MPa with a loss modulus of 4.8 MPa, and the storage modulus of a combination of 90 % volume ratio PMMA with 10 % volume ratio polyethylene oxide was 887.0 MPa, with a loss modulus of 597.0 MPa, at an imprint temperature of 100 °C using DMA data from previous research.

3. Fabrication methods

The fabrication carried out in this study consisted of two processes: the “multi-step imprinting process” and the subsequent “in-plain compression method.” Diagrams of both processes are shown in Figs. 6 and 7, respectively.

The 2-step imprinting was carried out first. The sample was set in a thermo-hygrostat at a temperature of 30.0 °C and a humidity of 80.0 % before imprinting. The humidity is important because the formation of the compound sheet depends on the water content; the formability was found to differ in preliminary experiments where the humidity was not constant, confirming that control of the water content in compound sheets is important. Imprinting was performed in a metallic container that was heated to 100 °C using a line-and-space-patterned mold with a pitch of 10 μm and

a groove depth of 10 μm [Fig. 6 (i)]. A servo-pressing machine was used to control the imprint stroke, and the applied load was measured using a load cell. The sample was then removed from the container and placed in a thermo-hygrostat at a temperature of 25.0 °C and a humidity of 50.0 % for 3600 s after which the sheet was removed from the mold. A spin coater was then utilized to apply a protective or sacrificial layer onto the surface of the compound sheet [Fig. 6 (ii)], and the sample was set in an oven to remove the solvent from the protective layer. Finally, the second imprint was made using the rougher mold [Fig. 6 (iii)]. The mold pattern used was a sinusoidal-like wavy shape with a pitch width of 130 μm and a groove depth of 65 μm. The imprint temperature was set to 100 °C. A hierarchical multi-scale pattern, in which there was a notable difference in size between the fine pattern and the rough pattern, was obtained via this process.

Next, the in-plane compression method was carried out in order to obtain higher aspect ratios of the imprinted product. The key factor in this process is compression, which is achieved via the elastic recovery of a silicone substrate. In this experiment, the elastic recovery force of a pre-tensioned silicone rubber substrate was used to create the compression, using the following method. First, the silicone rubber substrate (a silicone sheet of 0.3 mm thickness, AS ONE) was pre-tensioned according to the compression ratio. Next, the imprinted sheet was bonded to the silicon substrate using adhesive (Super-X2, Cemedine) that became rubbery after solidification. A primer (PPX-3, Cemedine) was also applied to improve the adhesion. After curing for 300 s, the sample was heated to 100 °C using an incandescent lamp, in order to soften the imprinted sample. The load applied to the silicone rubber was then released by changing the length of the substrate to the specified value. The sample was then compressed via the elastic recovery force. The experimental setup for this method is shown in Fig. 8. A linear actuator was used for precise control of the elongation.

4. Results and Discussion

The differences in the pattern at the interface due to the difference in the type of material used for the protective layer was first compared. In Fig. 9, cross sectional SEM images of the samples after the 2-step imprinting process are shown. The upper layers were constructed using PVA and PMMA. The mold pattern was transcribed onto the top surface of both samples, while the interfacial patterns were different. The interface of the sample in which PVA was used was almost planar, and only the fine pattern formed by the first imprint was deformed via the flow of the upper layer [Fig. 9 (a)]. In the sample in which PMMA was used, the interface followed the deformation of the surface layer, and the pattern formed by the first imprint was retained, as seen in Fig. 9 (b). As shown in Fig. 5, the PVA was easier to deform at 100 ˚C, meaning that the lower layer was not deformed in the same way when PVA was used.

The fine pattern was deeper in the sample with the PVA layer than in the sample where the PMMA layer was used. The interface of the sample with the PMMA layer was more deformed and

the length of the interfacial pattern was stretched. It is suggested that this stretched interface might cause the greater depth seen in the fine pattern using this material.

Next, the thickness of the protective layer was varied. In this experiment, differences in the thickness of the PMMA protective layer were generated by changing the maximum spin coating speed. Layers of 20 and 35 μm thickness were thus prepared. In Figs. 10(a) and (b), cross sectional SEM images of the samples with the 20 and 35 μm layers, respectively, are shown. The shape of the surface pattern of the protective layer matches that of the rough mold in both cases. Different shapes were observed at the interface of the thicker and thinner samples. The thicker upper layer prevented deformation in the lower layer. The effect of in-plane compression on the shape at the interface of the hierarchical multi-scale pattern was also confirmed. An SEM image of the sample with a thickness of 35 μm after in-plane compression is shown in Fig. 11. In this experiment, in-plane compression was carried out with a compression ratio of 1.5. The aspect ratio of the interfacial pattern is defined as height by pitch. The height and pitch are shown as the yellow and red arrows in Fig. 10. The aspect ratio of the above data is summarized in Fig. 12. The aspect ratio of the interface pattern was found to increase when in-plane compression was used, without destroying the fine pattern. To obtain a higher aspect ratio, it might be possible to prepare a mold with a higher aspect ratio for the second imprint. However, the fine pattern on the interface could easily be destroyed during a second imprinting [22], which is schematically shown in Fig. 3(b). From the above results, it is apparent that both controlling the thickness of the upper layer and using in-plain compression are essential to achieve higher aspect ratios.

For future studies, we plan to employ the proposed process using nanoscale patterns, in order to realize structural colors. A computational system could be a powerful tool in designing the parameters used in the process. From the DMA data of the materials (Fig. 5), the storage and loss moduli were influenced by both temperature and humidity when using PVA, as it is water-soluble. These data would be useful in developing a computational system such as FEM [32].

5. Summary

In this study, we proposed a new method for the fabrication of hierarchical multi-scale patterns with a high aspect ratio by combining multi-step imprinting with the in-plane compression method. The material used and thickness of the protective layer was changed, and the cross-sectional views of the samples were compared in order to investigate the effects of multi-step imprinting on the interface pattern. In-plane compression was carried out on the imprinted sample. The aspect ratio of the hierarchical multi-scale interfacial pattern was found to increase by both, thinning the protective layer and using the in-plane compression method.

Acknowledgements

This research is supported by the Adaptable and Seamless Technology transfer Program through Target-driven R&D (A-STEP) from the Japan Science and Technology Agency(JST). The research is also financially supported by the Mitsui Foundation for the Advancement of Tool and Die Technology.

References

1) S. Kinoshita, S. Yoshioka, and K. Kawagoe, Proc. R. Soc. B Biol. Sci. **269**, 1417 (2002).
2) X. Zhu, W. Yan, U. Levy, N. A. Mortensen, and A. Kristensen, Sci. Adv. **3**, e1602487 (2017).
3) W.-G. Bae, H. N. Kim, D. Kim, S.-H. Park, H. E. Jeong, and K.-Y. Suh, Adv. Mater. **26**, 675 (2014).
4) H. Lee, B. P. Lee, and P. B. Messersmith, Nature. **448**, 338 (2007).
5) F. Zhang, J. Chan, and H. Y. Low, Appl. Surf. Sci. **254**, 2975 (2008).
6) M. Yoshino, N. Umehara, and S. Aravindan, Wear, 266, 581 (2009).
7) P. B. Weisensee, E. J. Torrealba, M. Raleigh, A. M. Jacobi, and W. P. King, J. Micromech. Microeng. **24**, 095020 (2014).
8) A. Y. Vorobyev and C. Guo, J. Appl. Phys. **117**, 033103 (2015).
9) H. Kikuta, J. Jpn. Soc. Precis. Eng. **74**, 781 (2008).
10) L. Zhang, Z. Zhou, B. Cheng, J. M. DeSimone, and E. T. Samulski, Langmuir. **22**, 8576 (2006).
11) S. Y. Chou, J. Vac. Sci. Technol. B **14**, 4129 (1996).
12) S. Y. Chou and P. R. Krauss, Microelectron Eng. **35**, 237 (1997).
13) S. Y. Chou, P. R. Krauss, and P. J. Renstrom, Appl. Phys. Lett. **67**, 3114 (1995).
14) S. Y. Chou, P. R. Krauss, and P. J. Renstrom, Science **272**, 85 (1996).
15) L. J. Guo, Adv. Mater. **19**, 495 (2007).
16) Y. Xu, F. Tsumori, T. Toyooka, H. Kotera, and H. Miura, Jpn. J. Appl. Phys. **50**, 06GK11(2011).
17) F. Tsumori, Y. Tanaka, Y. Xu, T. Osada, and H. Miura, Jpn. J. Appl. Phys., (2014).
18) F. Tsumori, S. Hunt, K. Kudo, T. Osada, and H. Miura, J. Jpn. Soc. Powder Powder Met. **63**, 511 (2016).
19) F. Tsumori, Y. Xu, Y. Tanaka, T. Osada, and H. Miura, Procedia Engineer., 1433 (2014).
20) F. Tsumori, S. Hunt, T. Osada, and H. Miura, Jpn. J. Appl. Phys. **54**, 06FM03 (2015).
21) Y. Xu, F. Tsumori, H. G. Kang, and H. Miura, Adv. Sci. Lett. **12**, 170 (2012).
22) F. Tsumori, L. Shen, T. Osada, and H. Miura, Manuf. Rev. **2**, 10 (2015).
23) Y. Xu, F. Tsumori, H. G. Kang, and H. Miura, J. Jpn. Soc. Powder Powder Met. **58**, 673(2011).
24) Y. Xu, F. Tsumori, T. Osada, and H. Miura, Micro Nano Lett., 2013, p. 571.
25) F. Tsumori, K. Tokumaru, K. Kudo, T. Osada, and H. Miura, J. Jpn Soc. Powder Powder Met. **63**, 519 (2016).
26) K. Tokumaru, F. Tsumori, K. Kudo, T. Osada, and K. Shinagawa, Jpn. J. Appl. Phys., 06GL04 (2014).

27) B. Redha, S. H. Lim, M. S. M. Saifullah, and U. Kulkarni, Sci. Rep., 3, 1078 (2013).
28) F. Zhang and H. Y. Low, Nanotechnol., **17**, 1884 (2006).
29) K. P. Plucknett, C. H. Caceres, C. Hughes, and D. S. Wilkinson, J. Ame. Cer. Soc., 77, 2145 (1994).
30) Y. Hirai, M. Fujiwara, T. Okuno, Y. Tanaka, M. Endo, S. Irie, K. Nakagawa, and M. Sasago, J. Vac. Sci. Technol. B **19**, 2811 (2001).
31) C. H. Lin and R. Chen, J. Micromech. Microeng. **17**, 1220 (2007).
32) F. Tsumori, Y. Xu, H. Kang, T. Osada, H. Miura, Proc. COMPLAS, 1267 (2013).

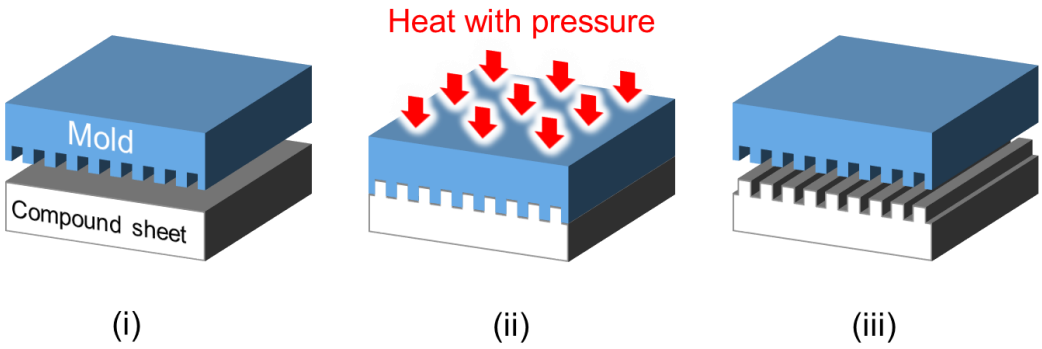

Fig. 1 Diagram of a typical thermal imprinting process. (i) A mold and a sheet are prepared. (ii) The sheet is simultaneously pressed and heated while using the mold. (iii) The mold is removed.

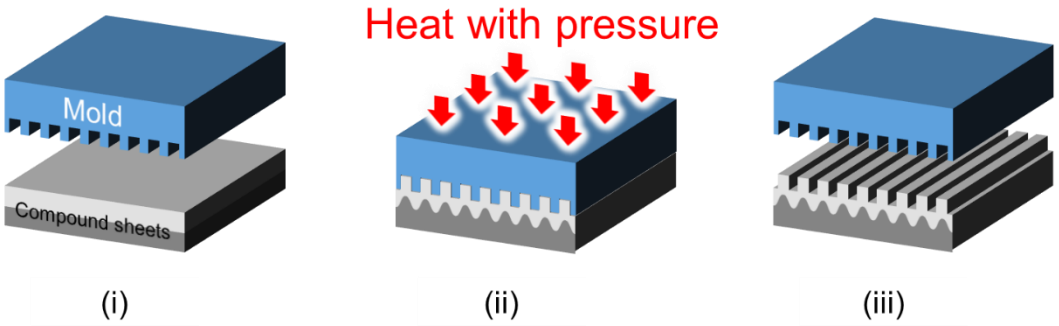

Fig. 2 Diagram of the thermal multi-layer imprinting process. A layered sheet is pressurized, forming not only a surface pattern but also an interfacial pattern.

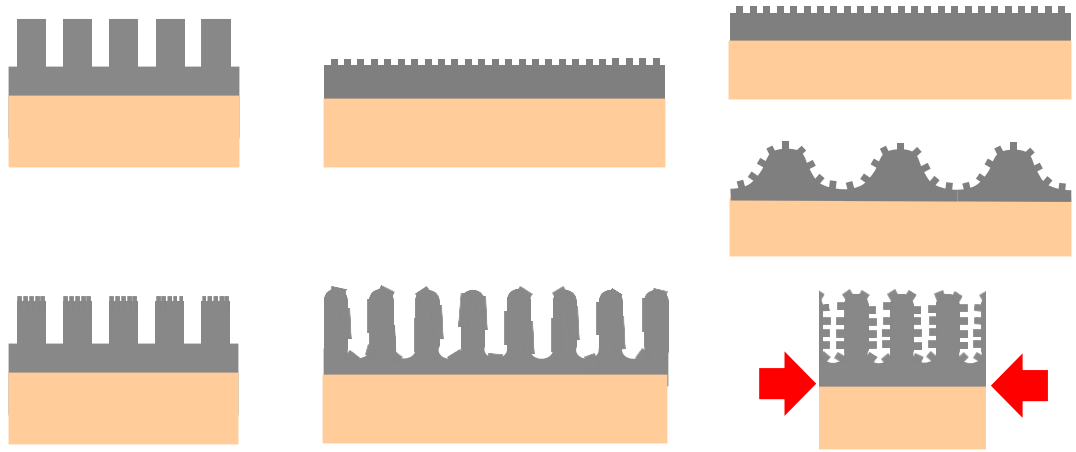

Fig. 3 Schematic illustration of the imprinting processes for hierarchical patterns. (a) A rough pattern is imprinted, but a finer pattern forms on the top [27, 28]. (b) A fine pattern is initially imprinted. However, the pattern is stretched and deformed after the second imprinting. (c) The strategy used in this study. A rough pattern with a low aspect ratio is formed, after which in-plane compression is performed.

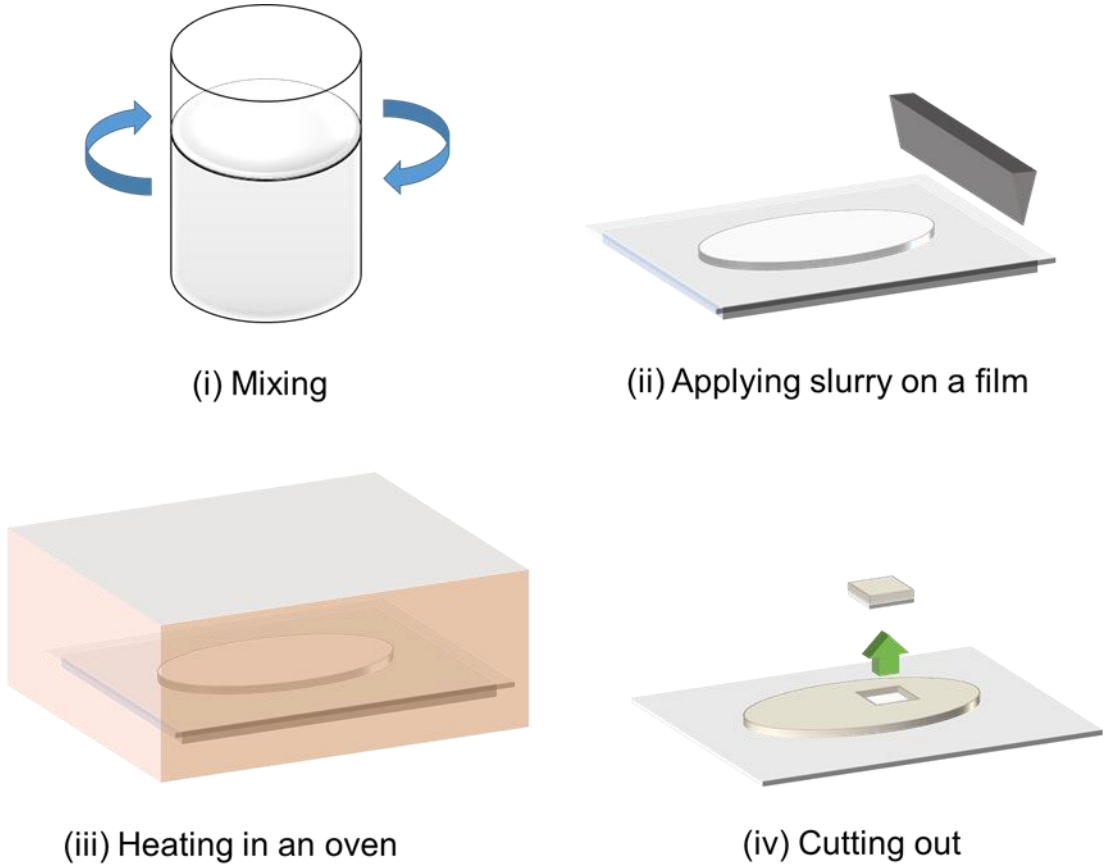

Fig. 4 Sequential preparation of the compound sheets for imprinting.

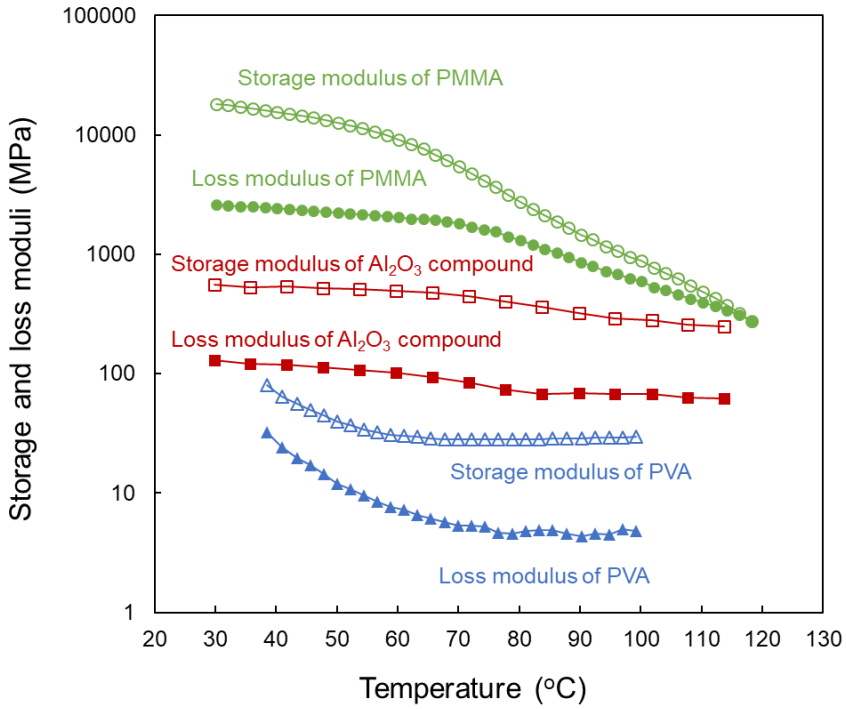

Fig. 5 Temperature dependence of the storage and loss moduli of the PMMA, PVA, and Al_2O_3 compound materials.

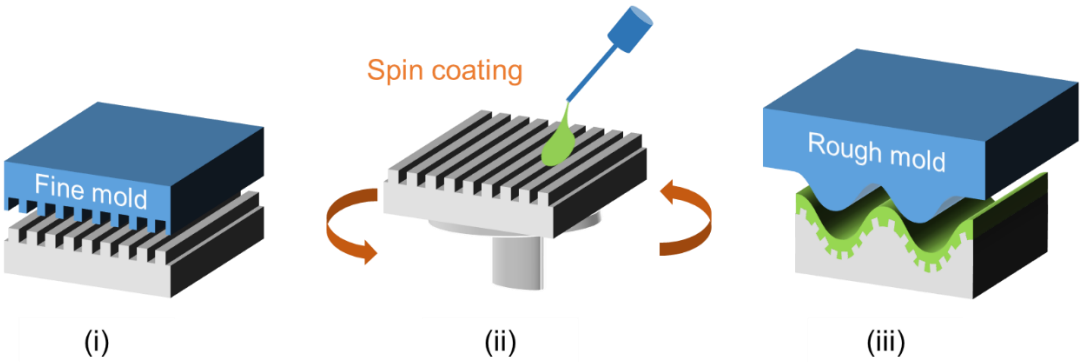

Fig. 6 Diagram of the proposed multi-step imprinting process; (i) Imprinting is carried out using a fine mold; (ii) A protective layer is applied by spin coating; and (iii) Imprinting is carried out with a rougher mold.

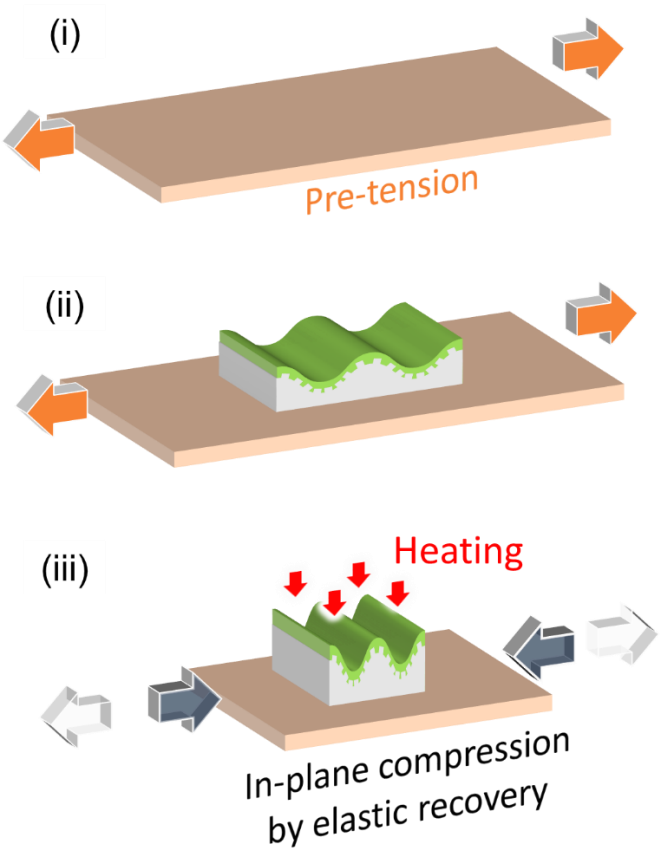

Fig. 7 Diagram of the in-plane compression method; (i) Elastic substrate is pre-tensioned; (ii) Imprinted sample is adhered onto the substrate; and (iii) The sample is deformed in-plane with the elastic recovery of the substrate.

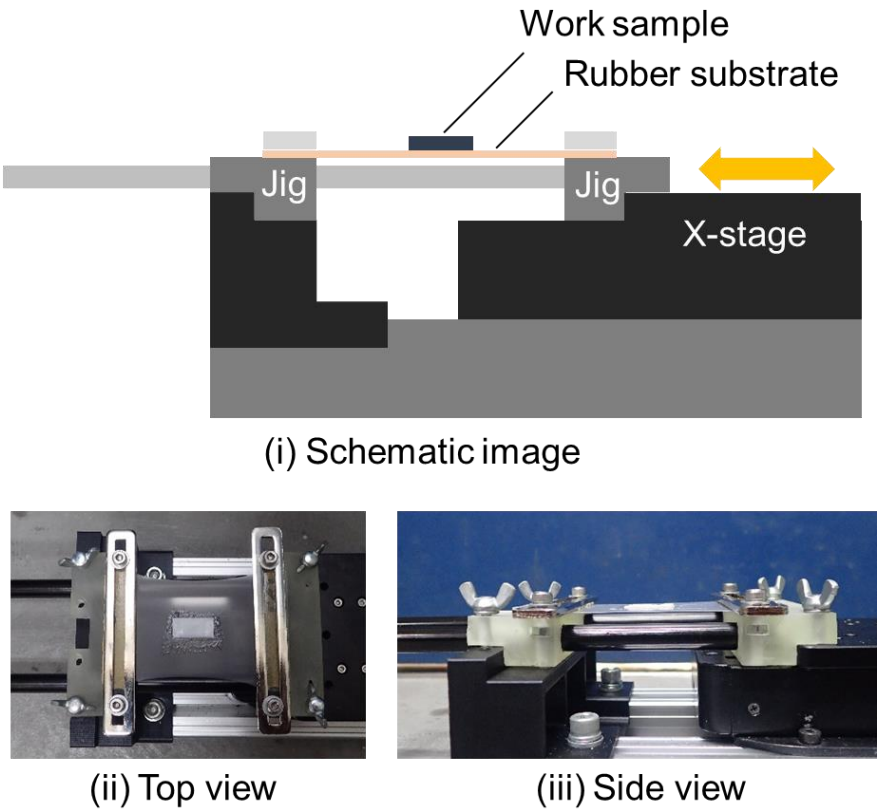

Fig. 8 Setup for the in-plane compression method; (i) Schematic diagram; (ii) Top view; and (iii) Side view of the device.

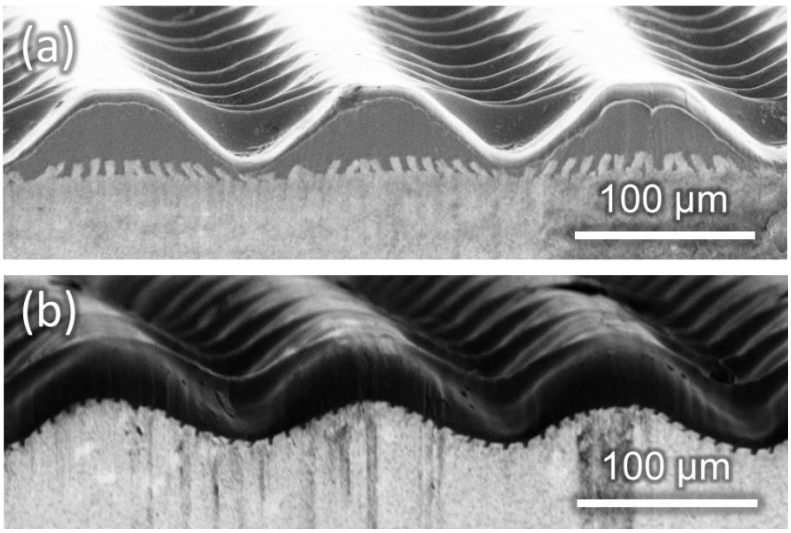

Fig. 9 Cross-sectional images of the multi-step imprinted samples using (a) PVA and (b) PMMA.

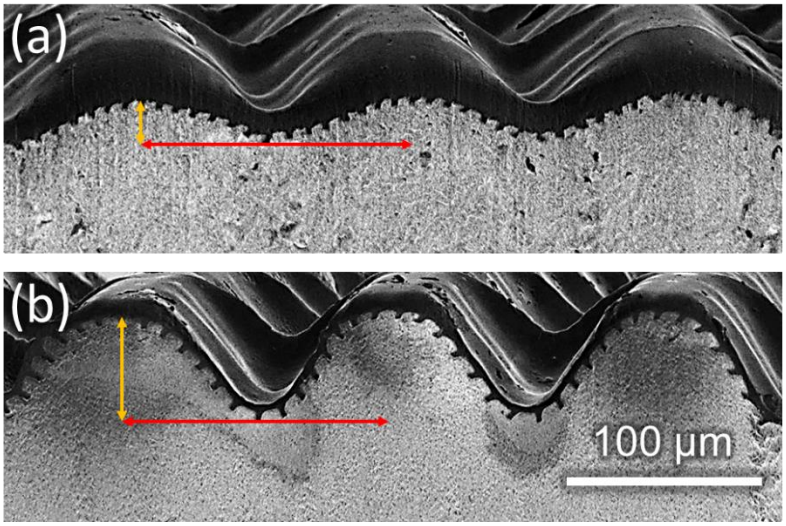

Fig. 10 Cross-sectional images of the molded product with (a) a thicker upper layer, and (b) a thinner upper layer.

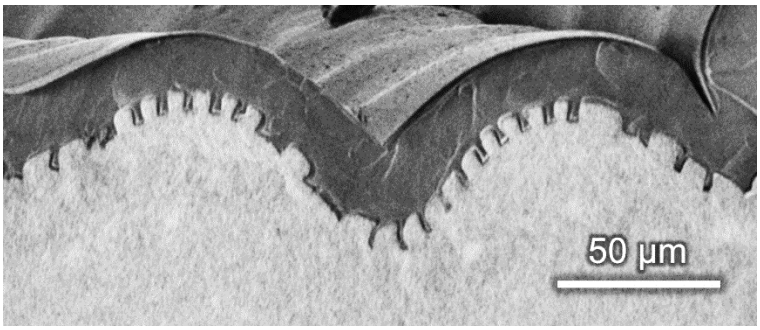

Fig. 11 Cross-sectional SEM image of the imprinted sample after in-plane compression.

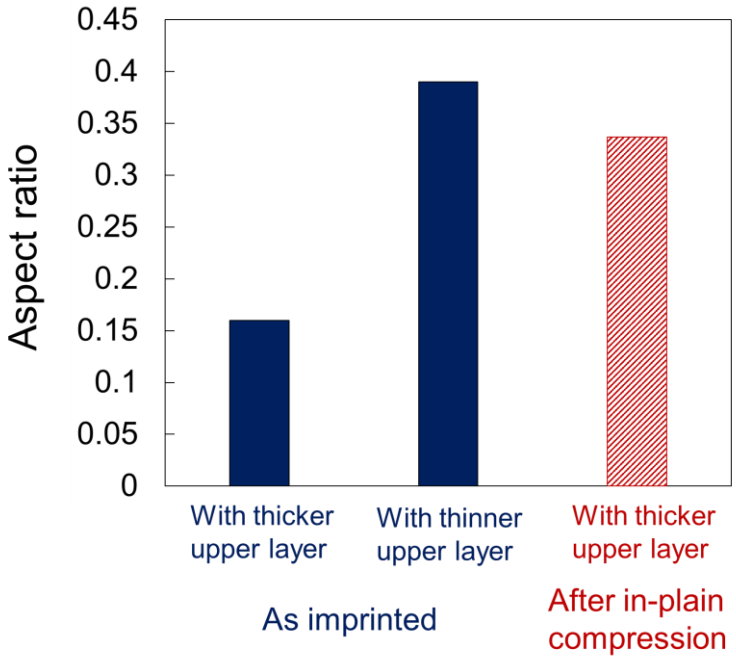

Fig. 12 Aspect ratio of the interfacial patterns of the three samples. The aspect ratio was larger where imprinting was carried out with a thinner upper layer. The aspect ratio also increased after in-plain compression.